Lawrence Berkeley National Laboratory

Title
A new approach to zip-lignin: 3,4-dihydroxybenzoate is compatible with lignification

Permalink
https://escholarship.org/uc/item/8md410zd

Journal
New Phytologist, 235(1)

ISSN
0028-646X

Authors
Unda, Faride
Mottiar, Yaseen
Mahon, Elizabeth L
et al.

Publication Date
2022-07-01

DOI
10.1111/nph.18136

Peer reviewed

A new approach to zip-lignin: 3,4-dihydroxybenzoate is compatible with lignification

Faride Unda[1,2] (iD), Yaseen Mottiar[1,2] (iD), Elizabeth L. Mahon[1,2] (iD), Steven D. Karlen[2,3] (iD), Kwang Ho Kim[1,4] (iD), Dominique Loqué[5] (iD), Aymerick Eudes[5,6] (iD), John Ralph[2,3] (iD) and Shawn D. Mansfield[1,2] (iD)

[1]Department of Wood Science, University of British Columbia, 2424 Main Mall, Vancouver, BC V6T 1Z4, Canada; [2]Department of Energy, Great Lakes Bioenergy Research Center, Wisconsin Energy Institute, University of Wisconsin-Madison, 1552 University Avenue, Madison, WI 53726, USA; [3]Department of Biochemistry, University of Wisconsin-Madison, 433 Babcock Drive, Madison, WI 53706, USA; [4]Clean Energy Research Center, Korea Institute of Science and Technology, Seoul 02792, Korea; [5]Joint BioEnergy Institute, 5885 Hollis Street, Emeryville, CA 94608, USA; [6]Environmental Genomics and Systems Biology Division, Lawrence Berkeley National Laboratory, Berkeley, CA 94720, USA

Author for correspondence:
Shawn D. Mansfield
Email: shawn.mansfield@ubc.ca

Summary

- Renewed interests in the development of bioenergy, biochemicals, and biomaterials have elicited new strategies for engineering the lignin of biomass feedstock plants. This study shows, for the first time, that 3,4-dihydroxybenzoate (DHB) is compatible with the radical coupling reactions that assemble polymeric lignin in plants.
- We introduced a bacterial 3-dehydroshikimate dehydratase into hybrid poplar (*Populus alba* × *grandidentata*) to divert carbon flux away from the shikimate pathway, which lies upstream of lignin biosynthesis.
- Transgenic poplar wood had up to 33% less lignin with *p*-hydroxyphenyl units comprising as much as 10% of the lignin. Mild alkaline hydrolysis of transgenic wood released fewer ester-linked *p*-hydroxybenzoate groups than control trees, and revealed the novel incorporation of cell-wall-bound DHB, as well as glycosides of 3,4-dihydroxybenzoic acid (DHBA). Two-dimensional nuclear magnetic resonance (2D-NMR) analysis uncovered DHBA-derived benzodioxane structures suggesting that DHB moieties were integrated into the lignin polymer backbone. In addition, up to 40% more glucose was released from transgenic wood following ionic liquid pretreatment and enzymatic hydrolysis.
- This work highlights the potential of diverting carbon flux from the shikimate pathway for lignin engineering and describes a new type of 'zip-lignin' derived from the incorporation of DHB into poplar lignin.

Introduction

Lignin is a phenolic polymer found predominantly in the secondary cell walls of xylem vessels, tracheids, and fibres where it plays crucial roles facilitating water transport and providing structural support to plants. Lignin is assembled primarily from three 4-hydroxycinnamyl alcohols known as monolignols – *p*-coumaryl, coniferyl, and sinapyl alcohols – which form the *p*-hydroxyphenyl (H), guaiacyl (G), and syringyl (S) subunits of lignin, respectively (Boerjan *et al.*, 2003). Following biosynthesis in the cytosol via the general phenylpropanoid pathway, lignin monomers are then exported to the cell wall and, once oxidized by laccase and/or peroxidase enzymes, undergo radical coupling reactions to form polymeric lignin (Freudenberg & Neish, 1968; Ralph *et al.*, 2004).

The molecular processes underpinning lignin formation are highly flexible and it has been shown that various noncanonical monomers are compatible with lignification. Among these are the acylated monolignol conjugates that result in ester-linked

acetate, benzoate, *p*-hydroxybenzoate, *p*-coumarate, and ferulate (Nakamura & Higuchi, 1976; Ralph & Lu, 1998; Lu & Ralph, 2002; Wilkerson *et al.*, 2014; Karlen *et al.*, 2016; Kim *et al.*, 2020; Goacher *et al.*, 2021); pathway intermediates such as hydroxycinnamaldehydes, caffeyl alcohol, and 5-hydroxyconiferyl alcohol, (Kim *et al.*, 2000; Ralph *et al.*, 2001; Kim *et al.*, 2003) and even phenolic compounds arising from outside the monolignol biosynthetic pathway such as flavonoids, hydroxystilbenes, and hydroxycinnamamides (del Río *et al.*, 2012, 2018, 2020; Lan *et al.*, 2015; Mahon *et al.*, 2021).

Woody feedstocks represent an abundant and fast-growing source of lignocellulosic biomass for use in the production of pulp and paper, biofuels, biomaterials, and biochemicals (de Vries *et al.*, 2021). Genetic engineering of economically important feedstock species is an attractive and proven strategy for improving the efficiency of biomass utilization (Mahon & Mansfield, 2019). Moreover, by harnessing the plasticity of lignification, noncanonical monomers can become incorporated into lignin leading to polymers with improved digestibility and/or

high-value constituents (Sederoff *et al.*, 1999; Ralph *et al.*, 2004, 2008a; Vanholme *et al.*, 2012; Mottiar *et al.*, 2016; del Río *et al.*, 2020). Lignin engineering efforts have been further buoyed by advancements in lignin valorization, microbial strain engineering, and the utilization of lignin-derived phenols via metabolic upgrading to create high-value biochemicals (Beckham *et al.*, 2016).

In previous work, expression of a bacterial 3-dehydroshikimate dehydratase gene (*QsuB*) from *Corynebacterium glutamicum* in Arabidopsis (Eudes *et al.*, 2015) led to the conversion of 3-dehydroshikimic acid, an intermediate of the shikimate pathway, into 3,4-dihydroxybenzoic acid (hereafter denoted as DHBA, with DHB being used to denote the dihydroxybenzoate ester and the phenolic moiety present in lignin, and also known as protocatechuic acid). This intervention diverted carbon flux away from the production of phenylalanine and resulted in reduced lignin content and improved saccharification potential. Herein, we investigated the effects of heterologous expression of *QsuB* in the plastids of hybrid poplar (*Populus alba × grandidentata*). Not only did this strategy result in reduced lignin content and improved saccharification, but it also led to the participation of monolignol–DHB conjugates in lignification, resulting in pendent DHB moieties on the lignin as well as backbone-integrated DHB units, ultimately producing a novel type of 'zip-lignin'.

Materials and Methods

Detailed methodology describing the generation, selection, and cultivation of transgenic hybrid poplar trees, cell wall compositional analysis, wood density, lignin histology, and synthesis of the model benzodioxane compound is included in the Supporting Information (Methods S1).

Soluble phenolics

Sections (10-cm) of fresh, de-barked stems were cut into small pieces and ground in a mortar and pestle with liquid nitrogen. After freeze-drying overnight, 100-mg portions of ground xylem were weighed into small vials along with 1.5 ml of 80% methanol and 5 µl of 3,4,5-trimethoxycinnamic acid as an internal standard. Following a 15-min incubation at 70°C in a thermomixer (Eppendorf, Hamburg, Germany) at 750 rpm, the vials were centrifuged for 5 min at 15 900 *g*, and 400 µl of supernatant was aspirated into a fresh tube. This process was repeated four times to give a pooled supernatant of 1600 µl. A 200-µl aliquot of the pooled methanolic extract was transferred into a fresh vial along with 10 µl of 200 mM sodium hydroxide (NaOH) and evaporated to dryness in a vacuum centrifuge. Then, 300 µl of 1 M hydrochloric acid (HCl) was added to the residue, mixed by vortexing, and the vial was incubated at 95°C for 3 h, to which, after cooling, 800 µl of ethyl acetate was added. After mixing and removing the upper organic phase, the extraction was repeated with an additional 800 µl of ethyl acetate. The combined fractions were then evaporated to dryness using a vacuum centrifuge and the residue was resuspended in 300 µl of methanol.

Samples were then analyzed using high-pressure liquid chromatography (HPLC) (Summit; Dionex, Sunnyvale, CA, USA) equipped with a Symmetry C18 column (4.6 mm × 250 mm, 5 µm particle size; Waters Corp., Milford, MA, USA) and a PDA-100 photodiode array detector (Dionex). Separation of peaks was achieved using a flow rate of 0.7 ml min^{-1} with a gradient from 95% to 55% of eluent A (0.1% trifluoroacetic acid in water) in eluent B (0.1% trifluoroacetic acid in 3 : 1 acetonitrile : methanol) over 50 min, followed by a 10-min wash with 75% eluent B and re-equilibration of the column with 95% eluent A for 10 min. The peaks corresponding to DHBA and 3,4,5-trimethoxycinnamic acid were integrated at the ultraviolet (UV) maxima of 265 and 295 nm, respectively. The internal standard was used for normalization purposes, and a calibration curve enabled quantification of total DHBA in the methanolic extracts.

Cell-wall-bound phenolics

Cell-wall-bound phenolics were liberated following the same procedure used to release cell-wall-bound acetyl groups (see Methods S1) except that *o*-anisic acid was used as an internal standard. High-pressure liquid chromatography analysis was performed as described earlier for soluble phenolics. Peaks corresponding to *p*-hydroxybenzoic acid (*p*HBA), DHBA, and *o*-anisic acid were integrated at the UV maxima of 255, 265, and 298 nm, respectively. The internal standard was used for normalization purposes, and external calibration curves enabled quantification. For acid hydrolysis of the alkaline hydrolysate, 200 µl of the hydrolysate was transferred into a microcentrifuge vial and 10 µl of 200 mM NaOH was added. The solution was evaporated down to *c.* 20 µl, and 300 µl of 1 M HCl was added. The solution was incubated at 95°C for 3 h, and then 800 µl of ethyl acetate was added before the vials were mixed thoroughly by vortexing. The upper organic phase was transferred into a new tube and evaporated to dryness in a vacuum centrifuge at 45°C for 15 min. The pellet was resuspended in 300 µl of 80% aqueous methanol and analyzed by HPLC as described previously for soluble phenolics.

Identification of cell-wall-bound phenolics

Identification of phenolics released by alkaline hydrolysis (as well as further acid hydrolysis of the alkaline hydrolysates) was performed using a Nexara X2 UHPLC (Shimadzu Corp., Kyoto, Japan) equipped with a diode array detector and an Impact II Ultra-High Resolution Qq-Time-of-Flight mass spectrometer (Bruker Corp., Billerica, MA, USA). Separation of peaks was achieved using a Symmetry C18 column (4.6 mm × 250 mm, 5 µm particle size; Waters Corp.) with a flow rate of 0.7 ml min^{-1} and using a binary gradient starting at 95% of eluent A (0.1% formic acid in water) and held for 1 min, ramped to 45% of eluent B (0.1% formic acid in 3 : 1 acetonitrile : methanol) over 49 min, then ramped to 75% eluent B over 1 min, followed by a 9-min wash with 75% eluent B, ramped

back to 5% eluent B for re-equilibration of the column at 95% eluent A for 10 min.

High-resolution mass spectrometry (HRMS) chromatographs were acquired from m/z 50–1000 Da at an acquisition rate of 8 Hz with the electrospray-ionization source operating first in negative-ion mode and then later in positive-ion mode. The MS configuration was as follows: capillary voltage, +3.5 kV in negative mode (-4.5 kV in positive mode); nebulizing gas, nitrogen at 4 bar; temperature, 210°C; drying gas, nitrogen at 8 l min^{-1}; autoMSMS triggering with collision energies split 50 : 50 between 5.6 and 10.5 eV, transfer funnel RF1 at 200 Vpp, transfer funnel RF2 200 Vpp, hexapole RF at 100 Vpp, quadrupole ion energy at 4 eV, prepulse storage at 5 µs. The HRMS chromatograms were analyzed using BRUKER COMPASS DATAANALYSIS 5.1 (Bruker Corp.). Calibration of the MS detector was performed independently for each sample using 10 mM sodium formate in 50 : 50 isopropanol : water, which was injected directly into the MS and eluted between 0.7 and 0.72 min. Chemical formulae for target masses were determined using the SmartFormula algorithm with formulae of $C_xH_yO_z$.

Nuclear magnetic resonance (NMR) was next used to confirm the identity of the MS-based assignments of the major peaks from the alkaline hydrolysates. The peaks were isolated using a two-step strategy. First, the NaOH and a portion of the background matrix was removed by size exclusion chromatography (SEC). A fresh batch of alkaline hydrolysate was prepared using a scaled-up version of the alkaline hydrolysis treatment (1 g extractive-free *QsuB*-poplar line 15 in 5 ml of 2 M NaOH). Then, following pelleting and filtration through a 0.2-µm nylon syringe filter, the sample was injected in 500-µl aliquots onto an SEC column (PolarSil analytical linear S, 8 mm × 300 mm, 5 µm partial size; PSS GmbH, Mainz, Germany) preconditioned with deionized water, at a flow rate of 1 ml min^{-1}. The eluent containing the phenolic fraction, as determined by absorption at 255 nm, was collected, pooled across the runs, and the water was removed using a rotary evaporator. The product mixture was then reconstituted in 2 ml of deionized water, filtered through a 0.2-µm nylon syringe filter, and the target peaks were isolated by HPLC. For peak isolation, the HPLC was equipped with a semi-prep C18 column (Phenomenex, Torrance, CA, USA). The mobile phase was pumped at 2 ml min^{-1} with a gradient elution program ramping from 99% of eluent A (0.1% formic acid in water) and held for 1 min, ramped to 45% of eluent B (0.1% formic acid in 3 : 1 acetonitrile : methanol) over 49 min, then ramped to 75% eluent B over 1 min, followed by a 9-min wash with 75% eluent B, and finally ramped back to 1% eluent B for re-equilibration of the column at 99% eluent A for 10 min. The combined SEC-purified sample was injected onto the column in 500-µl aliquots, and the elution bands were collected manually according to the chromatogram profile at 255 nm. To stabilize the acid-sensitive glycosylated products, a few drops of triethylamine were added to the collection tubes to ensure an alkaline pH. After removing the eluent using a rotary evaporator, samples were dissolved in 0.4 ml of either methanol-d_4 or acetone-d_6 and characterized by NMR. The identities of the major peak fractions were determined from HRMS, one-dimensional (1D)-, and two-dimensional (2D)-NMR pulse experiments, and by consulting published literature.

Enzyme-lignin preparation

Dried stems were ground and sieved to a particle size of 1 to 3 mm prior to solvent extraction, ball milling, and enzyme-lignin preparation, as described previously (Mansfield *et al.*, 2012). Extractives were removed by sonicating biomass samples sequentially in 80% ethanol (3 × 20 min), acetone (1 × 20 min), 1 : 1 chloroform : methanol (v/v, 1 × 20 min), and finally acetone (1 × 20 min). Extractive-free biomass was then ball-milled for 3 h per 500 mg of sample (with cycles of 10 min followed by 10 min rest) using a PM100 rotary ball mill (Retsch, Newtown, PA, USA) vibrating at 600 rpm in zirconium dioxide vessels (50 ml) containing zirconium dioxide ball bearings (20 × 6.5 mm diameter). Ball-milled samples were digested over 3 d at 50°C in 50 mM sodium citrate buffer (pH 4.8) containing Cellic CTec3 and HTec3 enzyme cocktails (Novozymes, Bagsværd, Denmark). A fresh mixture of buffer and enzymes was added each day. The residual enzyme-lignin preparations were washed with deionized water and lyophilized overnight.

Gel-permeation chromatography

In order to assess the molecular weight distribution of lignin, gel-permeation chromatography (GPC) was performed on enzyme-lignin preparations using a Tosoh Ecosec HLC-8320 GPC instrument (Tosoh Bioscience, Tokyo, Japan) equipped with a UV detector at 280 nm and a PLgel 5 µm Mixed-D column (Agilent Technologies Inc., Santa Clara, CA, USA). Tetrahydrofuran was used as eluent at a flow rate of 1.0 ml min^{-1} and the column was maintained at 35°C. Polystyrene standards purchased from Agilent were used to develop a calibration curve which ranged from 162 to 29 150 g mol^{-1}. All enzyme-lignin samples were derivatized using acetic anhydride and pyridine (1 : 1, v/v) at 60°C for 4 h prior to analysis.

Two-dimensional (2D)-NMR

Heteronuclear single-quantum coherence (HSQC) NMR spectra of isolated enzyme-lignin (*c.* 30 mg in 600 µl deuterated dimethyl sulfoxide (DMSO-d_6)) were obtained on an Avance-600 MHz instrument (Bruker Corp.) using the Bruker standard pulse sequence 'hsqcetgpsi2.2' ('double inept transfer using sensitivity improvement, phase-sensitive using echo/antiecho-TPPI gradient selection, with decoupling during acquisition, using trim pulses in inept transfer, with gradients in back-inept'). HSQC experiments for the enzyme-lignin samples were carried out using the following parameters: acquisition from 10 to 0 ppm in F2 (^{1}H) with 2k data points (acquisition time, 128 ms) and 165 to 0 ppm

in F1 (^{13}C) with 256 increments (F1 acquisition time, 3.85 ms) of 200 scans with a 1-s interscan delay; the d_{24} delay was set to 1.72 ms (1/4J, J = 145 Hz) optimized for methines (singly-protonated carbons). The total acquisition time per sample was 16.5 h. Processing to 2k × 1k used typical matched Gaussian apodization (GB = 0.001, LB = −0.2) in F2 and Gaussian apodization (GB = 0.001, LB = −1) in F1 (without using linear prediction). Major resolved peaks for common lignin units (A = β-ether, B = phenylcoumaran, C = resinol) were assigned based on prior data for similar samples (Kim & Ralph, 2010; Mansfield *et al.*, 2012). The benzodioxane assignments were made from the synthesized model compound **BD** (see Supporting Information Methods S1 and Fig. S8). The central solvent peak was used as an internal reference (δ_C/δ_H DMSO-d_6 39.5/2.39 ppm).

For the benzodioxane model compound **BD** (*vide infra*), the compound was dissolved in 0.5 ml of DMSO-d_6. NMR spectra were acquired on a Biospin Avance III 500 MHz spectrometer (Bruker Corp.) equipped with a cryogenically cooled 5-mm ^{1}H/^{13}C-optimized triple-resonance (^{1}H/^{13}C/^{15}N) TCI gradient probe with inverse geometry (proton coils closest to the sample) using standard Bruker-preferred pulse sequences; for the HSQC, we used Bruker standard pulse sequence 'hsqcetgpsisp2.2', a phase-sensitive gradient-edited-2D HSQC using adiabatic pulses for inversion and refocusing (Kupče & Freeman, 1997). Assignment authentication was again via the usual combination of 1D- and 2D-NMR pulse experiments.

Saccharification

The saccharification potential was evaluated for ionic liquid-pretreated biomass followed by enzymatic hydrolysis. A 10 wt% biomass slurry was prepared by mixing 0.2 g of biomass with 1.8 g of cholinium lysinate ([Ch][Lys]; pH 10–10.5) in a 10-ml pressure tube (Ace Glass, Vineland, NJ, USA). The tubes were heated to 80°C in an oil bath at atmospheric pressure. After 1 h, the tubes were cooled to room temperature and 6 ml of deionized water was added to the reaction slurry. This mixture was transferred to a 50-ml tube and centrifuged at 1240 *g*. The solid fraction, consisting mainly of polysaccharides, was washed four times with deionized water (4 × 6 ml) to remove any residual [Ch][Lys], and then freeze-dried. The concentration and conditions for the cholinium lysinate treatment employed in this study, which was previously shown to work well with poplar biomass, is very basic (pH 10–10.5) and thus aids in the liberation of ester linkages, and is therefore an effective pretreatment.

Enzymatic hydrolysis of pretreated poplar samples was performed for 72 h in 5 ml of 50 mM citrate buffer (pH 4.8) using a 9 : 1 ratio of Cellic CTec3 and HTec3 (Novozymes) at an enzyme loading of 10 mg protein g^{-1} biomass. Saccharification was conducted at 50°C in a rotary incubator with continuous shaking. Glucose and xylose releases were quantified using an Agilent 1100 series HPLC (Agilent Technologies Inc.) equipped with a refractive index detector and an Aminex HPX-87H column (300 mm × 7.8 mm; Bio-Rad Labs, Hercules, CA, USA). The mobile phase was 5 mM sulfuric acid at a constant flow rate of 0.6 ml min^{-1} and the column temperature was maintained at 60°C.

Results

Transgenic poplar trees

Hybrid poplar (*Populus alba* × *grandidentata*; P39) was transformed with the *pTKan-pC4H::schl::qsuB* construct described previously by Eudes *et al.* (2015) using *Agrobacterium*-mediated transformation. Positive transformants were identified by PCR screening. After several weeks of growth in tissue culture, transcript abundance was determined by semi-quantitative PCR. Subsequently, six lines exhibiting a range of transgene transcript abundance were transferred to antibiotic-free media and multiplied to obtain a minimum of six clonally propagated trees per independent transformation event. The transgenic trees (hereafter referred to as *QsuB*-poplar) and corresponding wild-type (WT) controls were then transferred to the University of British Columbia glasshouse and, after 5 months of growth, relative transcript abundance was again examined on the glasshouse-grown trees using reverse transcription quantitative polymerase chain reaction (RT-qPCR). Transcripts were present in the xylem tissue of all transgenic lines, but not in WT trees, as expected (Fig. S1).

The diameters of the stems and the number of sylleptic branches were recorded (Table S1). The stems of most of the transgenic lines were significantly thinner in diameter compared to WT trees, except for line 5 which was phenotypically similar to WT trees and exhibited the lowest expression of the transgene relative to the other transgenic lines. The number of sylleptic branches also differed with the *QsuB*-poplar trees having between 4.8 to 9.4 times more than WT trees (Table S1). Overall, plant stature and growth were not affected in this glasshouse trial, as both WT and transgenic lines appeared to grow similarly (Fig. S2). The cut stems of the transgenic and WT trees were left to dry following harvesting. After 1 wk, the wood of the transgenic lines began to crack, shrink in size, and darken in color (Fig. S3). Further microscopic observations of the dried stem cross-sections of the *QsuB*-poplar lines showed a mild collapsed xylem vessel phenotype when compared to WT trees (Fig. S4). Measurements of wood density revealed an increase in all transgenic lines, likely reflecting the collapse of vessel elements during sample drying, which therefore manifested in denser dried wood (Table S1).

DHBA-containing metabolites

The total amount of soluble DHB/DHBA in xylem tissue was quantified following acid hydrolysis of methanolic extracts derived from freeze-dried stem tissue. No detectable amounts of DHBA were released from WT tissue and only trace amounts were detected from *QsuB*-poplar line 5. Otherwise, soluble DHBA ranged from 7144 and 11 554 µg g^{-1} in the xylem of transgenic *QsuB*-poplar (Fig. 1).
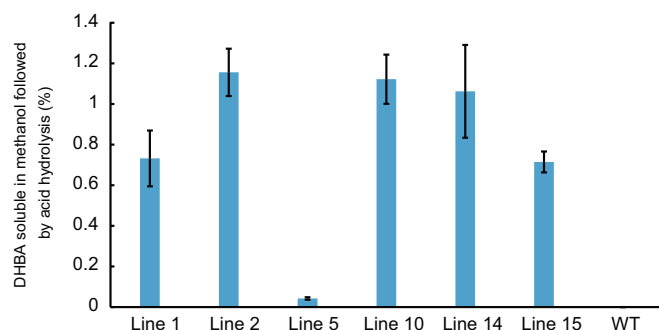
Fig. 1 Amount of methanol-soluble 3,4-dihydroxybenzoic acid (DHBA) in xylem tissue of *QsuB*-poplar and wild-type (WT) trees. Error bars represent the standard error of the mean of three biological replicates ($n = 3$). DHBA concentration was measured after acid-hydrolysis of the methanolic extracts to release its aglycone form.

Lignin and cell wall composition

The lignin content of extractive-free wood was determined using the Klason method. We observed significant reductions in total lignin content, with lines 15 and 1 containing 31% and 33% less lignin, respectively, compared to WT trees (Table 1). Additionally, thioacidolysis revealed a change in monomer composition. The proportion of S- and G-lignin monomers decreased significantly in the transgenic lines when compared to WT trees, whereas H-lignin units, which are typically detected only at trace levels in hybrid poplar, were especially prominent in *QsuB*-poplar (Table 1). Analysis of the carbohydrate composition of extractive-free wood showed no significant changes in glucose content. However, the xylose content increased significantly in many of the *QsuB*-poplar lines compared to both WT trees and the nonphenotypic *QsuB*-poplar line 5 (Table 1). Cell-wall-

bound acetyl groups liberated by alkaline hydrolysis increased by as much as 37% compared to WT trees, largely mirroring the increase in xylose levels (Table 1). Based on the lignin content and monomer composition, lines 1, 15, and 5 were chosen for further detailed characterization. Lines 1 and 15 were selected as severely and moderately phenotypic lines, respectively, whereas line 5 was chosen as a 'transgenic control', as it appeared to be most phenotypically similar to WT trees.

Cell-wall-bound phenolics

High-pressure liquid chromatography analysis of alkaline hydrolysates from extractive-free wood of *QsuB*-poplar and WT trees revealed differences in the accumulation of several compounds (Figs 2, S5). In addition to *p*-hydroxybenzoate (*p*HB), which is known to naturally decorate the lignin of xylem fibers in poplar (Goacher *et al.*, 2021), three new components apparent in the transgenic lines were identified as glycosides of DHBA (Fig. 2a,b, peaks 1, 3, 5). Furthermore, three additional compounds were identified as glycosides of 4-hydroxy-3-methoxybenzoic acid (vanillic acid) and 3-hydroxy-4-methoxy-benzoic acid (isovanillic acid) (Fig. 2a,b, peaks 2, 6, 8).

After acid hydrolysis of the alkaline hydrolysates, the three DHB-related peaks disappeared and the amount of free DHBA increased proportionately (Fig. 2a,b, peak 4). Similarly, the peaks related to 4-hydroxy-3-methoxybenzoate and 3-hydroxy-4-methoxybenzoate conjugates also disappeared with acid treatment to give free 4-hydroxy-3-methoxybenzoate and 3-hydroxy-4-methoxy-benzoate (Fig. 2a,b, peaks 9 and 10, respectively). Peaks 1 and 3 were assigned as the 4-*O*-glucoside and 3-*O*-glucoside of DHBA with HRMS masses of $[M - H]^- =$ 315.0728 and 315.0727 Da, respectively, and both compounds showed MS/MS fragmentation for the loss of hexose (162.0529)

Table 1 Cell wall analysis of transgenic *QsuB*-poplars and wild-type (WT) trees.

	Line 1	Line 2	Line 5	Line 10	Line 14	Line 15	WT
Klason lignin content (% w/w)							
Acid-insoluble lignin	**10.79 ± 0.26**	**13.53 ± 0.34**	16.26 ± 0.42	**12.94 ± 0.37**	**11.96 ± 0.33**	**11.66 ± 0.24**	17.08 ± 0.32
Acid-soluble lignin	**3.09 ± 0.07**	3.61 ± 0.22	3.75 ± 0.04	3.42 ± 0.15	3.61 ± 0.27	**2.76 ± 0.20**	3.82 ± 0.10
Total lignin	**13.88 ± 0.26**	**17.14 ± 0.51**	20.01 ± 0.46	**16.35 ± 0.52**0	**15.57 ± 0.12**	**14.42 ± 0.38**	20.90 ± 0.41
Lignin monomer composition (%)							
H units	**10.32 ± 0.45**	**6.40 ± 0.63**	nd	**6.49 ± 0.51**	**6.17 ± 0.56**	**10.87 ± 0.19**	nd
G units	**21.24 ± 0.40**	**23.94 ± 0.46**	28.45 ± 0.17	26.12 ± 0.76	**23.95 ± 0.50**	**20.58 ± 0.68**	27.08 ± 0.59
S units	**68.48 ± 0.52**	**69.66 ± 0.50**	71.55 ± 0.17	67.39 ± 0.77	**69.88 ± 0.31**	**68.55 ± 0.54**	72.92 ± 0.59
Structural polysaccharides (% w/w)							
Glucose	46.08 ± 0.85	44.73 ± 0.41	46.05 ± 0.21	46.08 ± 0.85	44.17 ± 0.48	45.50 ± 0.27	45.50 ± 0.16
Xylose	**20.54 ± 0.50**	**20.24 ± 0.19**	17.90 ± 0.38	**20.53 ± 0.31**	**21.06 ± 0.33**	**21.76 ± 0.14**	16.97 ± 0.14
Mannose	**0.98 ± 0.02**	**0.80 ± 0.08**	1.88 ± 0.07	**0.83 ± 0.05**	**0.91 ± 0.04**	**1.22 ± 0.06**	1.94 ± 0.10
Galactose	1.00 ± 0.06	1.09 ± 0.03	0.87 ± 0.06	1.09 ± 0.13	1.05 ± 0.13	0.81 ± 0.03	1.04 ± 0.11
Arabinose	0.37 ± 0.02	**0.42 ± 0.01**	0.34 ± 0.01	**0.42 ± 0.01**	**0.43 ± 0.02**	0.35 ± 0.00	0.32 ± 0.02
Rhamnose	0.51 ± 0.03	**0.56 ± 0.02**	0.49 ± 0.02	0.56 ± 0.03	0.52 ± 0.03	**0.51 ± 0.01**	0.45 ± 0.01
Cell-wall-bound acetyl (% w/w)							
Acetyl	**4.55 ± 0.30**	**4.25 ± 0.10**	3.40 ± 0.07	**4.18 ± 0.07**	**4.23 ± 0.03**	**4.17 ± 0.01**	3.32 ± 0.04

Lignin content and composition, structural polysaccharides composition, and acetyl content from extractive-free wood of 5-month-old trees. Values represent the average ± standard error of the mean for three biological replicates ($n = 3$). Values in bold are significantly different from WT using Student's *t*-test ($P < 0.01$). nd, not detected.
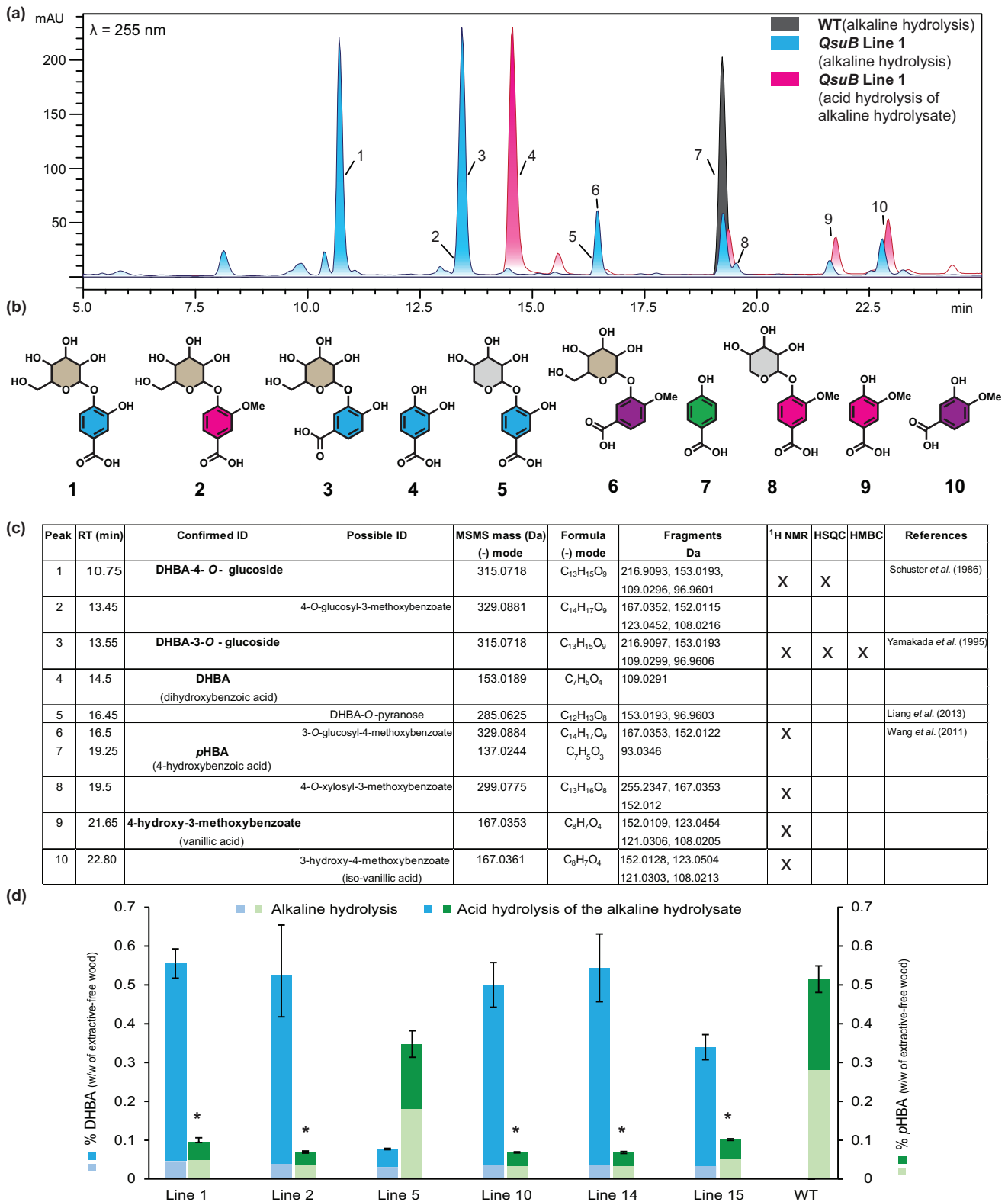
Fig. 2 Cell-wall-bound phenolics in the xylem tissue of *QsuB*-poplar and wild-type (WT) trees. (a) Ultrahigh-pressure liquid chromatography (UHPLC) traces of alkaline hydrolysates of extractive-free wood from *QsuB*-poplar line 1 (blue) and WT (grey). The trace of an alkaline hydrolysate subjected to acid hydrolysis is also shown for *QsuB*-poplar line 1 (pink). (b) Structure of compounds released by alkaline hydrolysis of extractive-free wood from *QsuB*-poplar line 1. (c) Compound identities, high-resolution mass spectrometry (HRMS) [M − H]⁻, chemical formulae, HRMS fragments, and nuclear magnetic resonance (NMR) analysis. (d) Amount of 3,4-dihydroxybenzoic acid (DHBA) and *p*-hydroxybenzoic acid (*p*HBA) released after alkaline hydrolysis and acid hydrolysis of the alkaline hydrolysates of extractive-free wood. Error bars represent the standard error of the mean ($n = 3$). Asterisks denote statistically significant differences from WT ($P < 0.01$; Student's *t*-test).

(Fig. 2c). We also observed the loss of a hexose (162.0529) to DHBA ([M − H]⁻ 153.0193) after acid hydrolysis of the alkaline hydrolysate, further supporting the phenolic glucoside assignment. Comparing the UV-visible spectrum of the DHBA 3-*O*-glucoside to that of the DHBA 4-*O*-glucoside showed a *c.* 4-nm red shift in the π–π* transition to 254 nm vs 250 nm, respectively, and a *c.* 4-nm blue shift in the *n*–π* transitions to shoulder at 287 nm vs the discrete peak at 291 nm (Fig. S6). The NMR spectra of the two compounds were also distinct allowing for the confirmation of the compound identities by comparisons with previously reported spectra obtained from synthetic standards (Schuster *et al.*, 1986; Yamanaka *et al.*, 1995). Another DHBA conjugate, peak 5 ([M − H]⁻ 285.0625 Da), exhibited a loss of xylose (132.0432) under MS/MS fragmentation to the DHBA fragment (153.0193), and this peak was absent after acid hydrolysis (Fig. 2c). We hypothesized that it corresponds to the DHBA *O*-xylopyranoside, which was previously reported from *Lysimachia clethroides* (Liang *et al.*, 2013).

Based on the HRMS data, we hypothesized that peak 2 corresponds to 4-*O*-glucosyl-3-methoxybenzoate with a mass of [M − H]⁻ of 329.0881 Da, whereas peak 6 with a similar HRMS [M − H]⁻ of 329.0884 Da corresponds to 3-*O*-glucosyl-4-methoxybenzoate (Fig. 2a–c). As peak 6 was chromatographically resolved from other major compounds, we were able to acquire a unique UV-visible spectrum (π–π* transition of 254 nm and the *n*–π* transitions at 287 nm as a shoulder) that closely matched that of the 3-*O*-glucoside of DHBA (Fig. S6). NMR analysis of peak 6 further supported this assignment with chemical shifts corresponding to those previously reported (Wang *et al.*, 2011). Additionally, peak 8 corresponds to 4-*O*-xylosyl-3-methoxybenzoate with a mass of 299.0775 Da. All three compounds (peaks 2, 3, and 8) were lost in acid hydrolysis releasing either a hexose (162.0529) or a xylose (132.0432 Da) and the 4-hydroxy-3-methoxybenzoate fragment (167.0353 Da). Furthermore, peak 9 (which was retained during acid treatment) was validated with authentic standards as 4-hydroxy-3-methoxybenzoate.

Identification of DHBA (peak 4) and *p*HBA (peak 7) by HRMS was also validated with authentic standards. Quantification of the extractive-free tissue (Fig. 2d) showed that the total cell-wall-bound DHB accumulated up to 5.07 mg g⁻¹ in *QsuB*-poplar line 15. All transgenic lines showed a significant reduction in *p*HB moieties (Fig. 2d).

Degree of polymerization of lignin and DHBA-derived benzodioxane units

The degree of polymerization of lignin isolated from *QsuB*-poplar and WT biomass following enzymatic hydrolysis was analyzed by GPC. The distribution curves of the molecular weights showed an increased abundance of lignin in the lower molecular weight range (< 7500 Da) and a decreased abundance of higher molecular weight lignin (> 10 000 Da) in *QsuB*-poplar lines 1 and 15 when compared to WT (Fig. 3).

Analysis of the same lignin (lignin isolated following enzymatic digestion with cell wall degrading enzymes) by 2D-NMR further
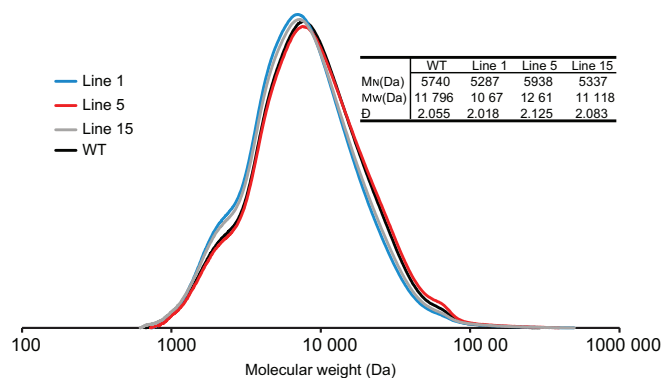

	WT	Line 1	Line 5	Line 15
M_N(Da)	5740	5287	5938	5337
M_W(Da)	11 796	10 67	12 61	11 118
Đ	2.055	2.018	2.125	2.083

Fig. 3 Gel-permeation chromatograms of cellulolytic enzyme-lignins. Values for number average of the molecular weight in Daltons (Da) (M_N), weight average of the molecular weight (M_W), and dispersity index (*Đ*) are indicated for *QsuB*-poplar lines and wild-type (WT) trees.

supported the results obtained by thioacidolysis and alkaline hydrolysis of the cell wall material (Fig. 4). Remarkably, α- and β-C/H correlations consistent with benzodioxane structures from the lignin of *QsuB*-poplar (by their identity with analogous peaks from the synthesized model compound) showed the presence of DHB, implying that not only do monolignol–DHB conjugates participate in radical coupling reactions during the formation of lignin, but the DHB moiety itself (unlike *p*HB, for example) is involved in radical coupling reactions. One of the C/H aromatic peaks corresponding to the benzodioxane signatures is clear in this region of the spectra (Fig. 4), whereas the other two peaks overlap with the large correlations from the normal G-lignin units (Figs S7, S8).

Saccharification potential

Finally, to assess how these changes in lignin chemistry may have affected cell wall recalcitrance, we performed saccharification assays on stem tissues of *QsuB*-poplar and WT trees. Ionic liquid ([Ch][Lys]) pretreatment was followed by enzymatic hydrolysis reactions. Saccharification potential was improved significantly in most of the transgenic lines, with lines 1 and 15 showing 31% and 40% more glucose release than WT, and line 15 releasing 33% more xylose than WT (Fig. 5).

Discussion

Lignin engineering with *QsuB*

Fast-growing and highly productive hardwood species such as eucalypts, poplars, and willows are abundant sources of lignocellulosic biomass, and have increasingly become targets for breeding and/or genetic modifications aimed at altering wood properties to improve the efficiency of industrial biomass utilization (Mahon & Mansfield, 2019; Murphy *et al.*, 2021). Gain-of-function approaches that not only reduce cell wall recalcitrance but which also impart additional value to biomass represent a particularly promising strategy to enable more cost-effective processing of woody biomass.
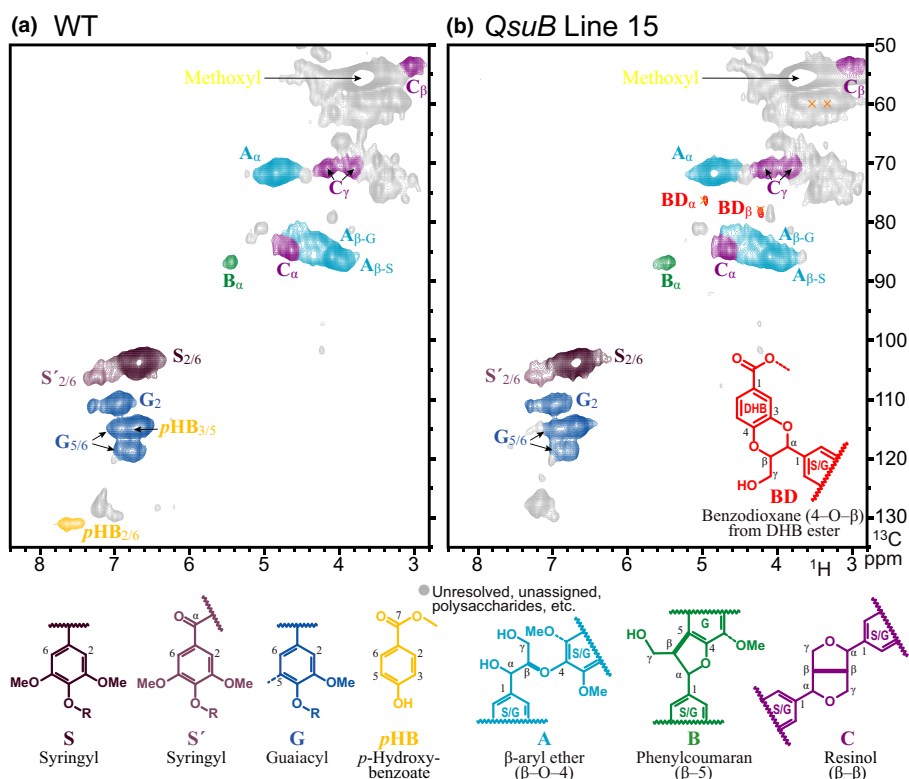
Fig. 4 Partial short-range proton–carbon-13 (^{1}H–^{13}C) heteronuclear single-quantum coherence (HSQC) nuclear magnetic resonance (NMR) spectra of the isolated enzyme-lignins from wild-type (WT) (a) and *QsuB*-poplar line 15 (b) poplar. The spectra show, color-coded to the structures below, the S and G units typical of a hardwood lignin and, in the WT, the pendent *p*-hydroxybenzoate (*p*HB) units acylating the lignin sidechain that is typical in poplar, and the main types of inter-unit linkages (A–C) in lignin. The *QsuB* line 15 lignin spectrum (b) has two notable features, the drastic reduction in levels of *p*HB groups, and fairly compelling evidence for the presence of 3,4-dihydroxybenzoate (DHB) units. Peaks matching those from the model compound BD (as shown in red, and by the orange ×) for each sidechain C/H pair are apparent in (b); the full data for the model are given in Supporting Information Fig. S7. As is usual for NMR, the evidence is not absolute but quite compellingly diagnostic given that four items of simultaneously matching data are evident – the carbon and proton shifts for each of the α and β positions characteristic of the benzodioxane from 3,4-dihydroxybenzoic acid (DHBA).
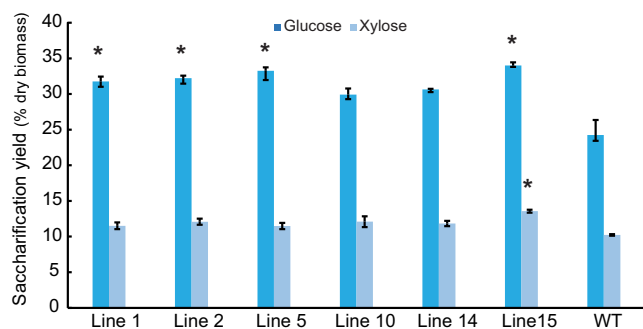

Fig. 5 Saccharification yield from wood of 5-month-old *QsuB*-poplar and wild-type (WT) trees. Pretreatment: 1 h at 80°C in cholinium lysinate [Ch] [Lys] (10% wt biomass loading). Pretreated biomass residue washed with water and subjected to enzymatic hydrolysis for 72 h with commercial cellulase and hemicellulase cocktails (statistically significant differences from WT *, $P < 0.01$; Student's *t*-test). Error bars represent the standard error of the mean ($n = 3$).

In this study, we transformed hybrid poplar with a bacterial 3-dehydroshikimate dehydratase gene (*QsuB*) that was previously shown to reduce lignin deposition and improve saccharification yields in Arabidopsis and switchgrass (Eudes *et al.*, 2015; Hao *et al.*, 2021). Expression of *QsuB* in hybrid poplar led to the

hyperaccumulation of soluble DHB in the xylem, and effectively diverted carbon flux away from the phenylpropanoid pathway resulting in decreased lignin content, altered lignin monomer composition, and improved saccharification potential compared to WT trees. Cell wall analysis of the *QsuB*-poplars showed that conjugated forms of DHBA were actually polymerized into the lignin leaving some DHB as ester-linked pendent groups. Moreover, the discovery of DHB-derived benzodioxane structures in the 2D-NMR spectra suggests that the DHB moieties of these conjugates can also participate in radical coupling reactions themselves leading to backbone-integrated DHB and the possibility of a new type of 'zip-lignin' resulting from the ester bonds derived from lignification using monolignol–DHB conjugates.

Hyperaccumulation of DHB in *QsuB*-poplar

Transgenic *QsuB*-poplar accumulated significant amounts of soluble DHB/DHBA, presumably as glycosylated forms (Fig. 1). DHBA produced *in planta* could be extracted as soluble compounds that can, for example, be further converted into *cis,cis*-muconic acid (*cc*MA), a precursor for chemicals such as adipic acid, terephthalic acid, and trimellitic acid, all of which are used in the production of various plastics and nylons (Xie *et al.*, 2014). Recent

studies have demonstrated that DHBA produced by genetically engineered tobacco expressing *QsuB* can be converted into *cc*MA using an engineered *Escherichia coli* strain (Wu *et al.*, 2017). Employing the same lignin-specific promoter, the *QsuB*-poplar lines in this study produced up to $11.5 \, \mathrm{mg \, g^{-1}}$ of extractable DHBA in xylem tissue (Fig. 1) compared to just 1.45, 0.133 and $0.375 \, \mathrm{mg \, g^{-1}}$ produced by *QsuB*-expressing tobacco, Arabidopsis, and switchgrass, respectively (Eudes *et al.*, 2015; Wu *et al.*, 2017; Hao *et al.*, 2021). Given the fast growth rates of hybrid poplar and the proven capacity to generate substantial amounts of DHB, these trees could prove to be useful as value-added woody feedstocks.

Incorporation of DHB conjugates into lignin

Lignin is synthesized via dehydrogenative polymerization driven by the radical coupling of, primarily, the three canonical monolignols *p*-coumaryl, coniferyl, and sinapyl alcohol. However, lignification is a highly flexible process and a growing number of noncanonical subunits have been reported in diverse plant taxa (del Río *et al.*, 2020). In this study, we have shown that *QsuB*-poplar trees not only accumulate DHB in the soluble fraction, but DHB conjugates were also incorporated into the lignin resulting in ester-linked DHB pendent groups, as well as lignin backbone-integrated units (Figs 2, 4).

Unlike in most other dicots, the lignin of poplar is abundantly decorated with *p*HB pendent groups, which are conjugated to monolignols in the cytosol prior to export to the cell wall space where the monolignol moieties of these conjugates radically couple into lignin, giving rise to free-phenolic pendent groups of *p*HB (Ralph, 2010). The biosynthesis of *p*HBA proceeds from *p*-coumarate, an intermediate of the general phenylpropanoid biosynthetic pathway (Loscher & Heide, 1994; Sircar & Mitra, 2008). By diverting carbon flux in the shikimate pathway away from the production of phenylpropanoids including *p*-coumarate, expression of *QsuB* in poplar evidently reduced the availability of *p*HBA for lignin acylation.

p-Hydroxybenzoylation of lignin occurs via the incorporation of acylated monolignols rather than by post-polymerization acylation (Lu *et al.*, 2015). And, the gene encoding this specific *p*-hydroxybenzoyl-coenzyme A (CoA) monolignol transferase has recently been identified and functionally tested in poplar in two independent studies (Zhao *et al.*, 2021; de Vries *et al.*, 2022). In *QsuB*-poplar, we observed significant reductions in *p*HBA released from the cell wall following alkaline hydrolysis. By contrast, several conjugates of DHBA were detected (Fig. 2), with several of these being glycosylated forms. It is plausible that these novel cell-wall-bound DHB groups could have arisen from the same monolignol transferase(s) that are normally responsible for the production of monolignol–*p*HB conjugates (Fig. S9). If so, our findings imply that these transferases possess significant promiscuity in substrate tolerance and that monolignol–DHB conjugates can be effectively exported to the cell wall and incorporated into lignin. Competition for the transferase between endogenous *p*HBA and excessive DHBA could also partly explain the observed decreases in cell-wall-bound *p*HB groups. Surprisingly, the glycosylated forms may also be

accepted by the transferase as these too occurred on the lignin of *QsuB*-poplar. In addition to the transferase, 4CL or 4CL-like enzymes must also then act on DHBA to produce the CoA thioester form (Fig. S9).

Alternatively, given that DHB esters can evidently participate in radical coupling reactions, it is possible that DHB esters other than those conjugated with a monolignol could be exported and incorporated into lignin without the involvement of any monolignol acyltransferases. As support for this hypothesis, cell wall analyses of the leaves of *Vitis vinifera* and the roots of *Ginkgo biloba* (both species that are not known to possess highly acylated lignin) showed that DHB can occur naturally in a cell-wall-bound form at low levels (Codignola *et al.*, 1989; Weber *et al.*, 1995). Whether or not DHB-acylation of lignin in *QsuB*-poplar is facilitated by monolignol acyltransferases is a question that will be best answered in due course using enzyme activity assays of the recently characterized *p*-hydroxybenzoyl-CoA monolignol transferase.

NMR analysis of *QsuB*-poplar lignin revealed signatures of DHB-derived benzodioxane structures (Fig. 4). As was observed in transgenic poplars expressing an exotic feruloyl-CoA monolignol transferase in which increased levels of readily cleavable ester bonds were incorporated into the lignin backbone (Wilkerson *et al.*, 2014), DHB evidently participates in radical coupling reactions and thereby incorporates into the backbone structure of lignin. Unlike *p*HB esters that prefer radical transfer over radical coupling reactions and thus occur as pendent groups in poplar, the second hydroxyl group of DHB appears to render it more compatible with the radical coupling reactions of lignification, leading to DHB units that integrally incorporate into the polymer.

Alkaline hydrolysis also revealed the presence of cell-wall-bound glycosides of 4-hydroxy-3-methoxybenzoate and 3-hydroxy-4-methoxybenzoate in *QsuB*-expressing poplar. As these compounds were absent from the alkaline hydrolysates of WT poplar, we postulate that they may have been produced directly from DHBA. This would involve one or more *O*-methyltransferase enzymes that methylate the *para* or *meta* hydroxyl groups of DHBA. Although none of the 26 *O*-methyltransferases in poplar has been specifically reported to have such activity, such enzymes are known to accept diverse phenolic substrates (Lam *et al.*, 2007; Barakat *et al.*, 2011). Indeed, nonspecific *O*-methyltransferase activity towards DHBA has been described previously in poplar and in various other plant taxa as well (Finkle & Masri, 1964; Kuroda, 1983).

Although we have not conclusively demonstrated their association with lignin, it is apparent that phenol-glycosylated monolignol–DHB esters can be incorporated into the cell wall. Phenols involved in radical coupling following one-electron oxidation ('radicalization') need to be in their free-phenolic form, but monomers or monomer conjugates in which other noncrucial phenolic groups are glycosylated can still enter lignification via the radical generated from the molecule's free phenolic group. As a precedent, hydroxystilbene glucosides were recently identified in the bark of Norway spruce (Rencoret *et al.*, 2019). We anticipate that future studies will uncover further examples of such lignin-bound sugars, particularly in plant tissues in which phenolic glycosides accumulate to high levels.

Effects on lignin and biomass recalcitrance

Targeted expression of *QsuB* in the plastids of lignifying xylem tissue diverts carbon flux away from the shikimate pathway and towards the production of DHBA. In transgenic Arabidopsis lines expressing *QsuB* there was no reduction in tryptophan, phenylalanine, tyrosine or salicylate, all downstream products of the shikimate pathway; even so, there was an accumulation of the precursors for the H lignin units (*p*-coumarate, *p*-coumaralde-hyde, and *p*-coumaryl alcohol) (Eudes *et al.*, 2015). In poplar, we found that heterologous expression of *QsuB* results in reduced lignin content and a significant accumulation of H-lignin units along with a higher S : G lignin monomer ratio compared to WT trees. Reduction of carbon flux into or within the phenyl-propanoid pathway often results in reduced overall lignin, combined with an increase in the S : G ratio, as metabolic flux into G-lignin is more severely impacted by a reduction in substrate availability (Wang *et al.*, 2014, 2018).

QsuB acts to divert carbon flux upstream of shikimate and, in so doing, could lead to a reduction in the pool of shikimate available during lignin biosynthesis. As *p*-hydroxycinnamoyl-CoA shikimate *p*-hydroxycinnamoyl transferase (HCT) requires shiki-mate as a co-substrate, a reduction in the available shikimate would clearly hinder the progression of monolignol biosynthesis beyond HCT leading to coniferyl and sinapyl alcohols (Bonawitz & Chapple, 2010). In this way, proportionately more *p*-coumaryl alcohol would be produced resulting in an increase in H-lignin units, as we saw with *QsuB*-poplar. In previous work, it has been shown that at least one poplar HCT can accept DHBA as a co-substrate instead of shikimate (Eudes *et al.*, 2016). While it remains to be seen whether the resulting *p*-coumaroyl–DHB is tolerated by coumarate 3-hydroxylase (C3′H, *p*-coumaroyl shiki-mate 3′-hydroxylase), and whether the ester moiety can be subse-quently released by HCT or caffeoyl shikimate esterase (CSE), this could provide another possible explanation for the altered flux through the metabolic grid that is monolignol biosynthesis.

In addition to compositional changes to lignin, we observed a reduced degree of polymerization (DP) in the lignin fraction of transgenic trees compared to WT controls. Reduced DP has been observed in lignin exhibiting higher amount of H units and has been proposed as an alternative strategy to improve saccharifica-tion efficiency (Ziebell *et al.*, 2010; Eudes *et al.*, 2012; Mottiar *et al.*, 2016). Altogether, the reductions in lignin content and DP likely played significant roles in improving saccharification yields by up to 40% for glucose and up to 33% for xylose.

Perspectives on lignin engineering

Perturbations of the phenylpropanoid pathway in poplar in pre-vious studies have often resulted in a reduction of total lignin accompanied by compensatory increases in cell wall polysaccha-rides, typically cellulose (Li *et al.*, 2003; Leplé *et al.*, 2007; Cole-man *et al.*, 2008b; Bjurhager *et al.*, 2010). Elevated levels of cellulose in low-lignin plants are generally assumed to be the result of increased carbon availability for polysaccharide biosyn-thesis. However, in *QsuB*-poplar we observed no increase in

glucose (i.e. cellulose), despite achieving comparable reductions in lignin content. *QsuB*-expressing lines displayed more xylose (i.e. xylan) in cell walls compared to WT. Increases in hemicellu-lose content and changes in hemicellulose composition have been reported in other low-lignin poplar trees (Coleman *et al.*, 2008a; Van Acker *et al.*, 2014), as well as in aspen mutants with reduced cellulose (Joshi *et al.*, 2011), all of which displayed an irregular xylem phenotype similar to *QsuB*-poplar.

Cell-wall-bound DHB evidently occurs in the lignin of *QsuB*-poplar in two forms: as ester-linked pendent groups, and as backbone-integrated units (Fig. S9). As mentioned earlier, the latter form introduces ester linkages directly into the backbone of lignin polymers to form zip-lignin structures. These alkali-labile linkages readily translate into improved biomass processability by rendering the lignin more amenable to chemical deconstruction. However, the pendent DHB groups also offer industrial advan-tages as these ester-linked moieties can be easily cleaved during processing. Once separated, these clip-off phenolics could be used as platform compounds in chemical or microbial upgrading to produce an array of high-value biochemicals. In this way, lignin engineering strategies such as that exemplified by *QsuB*-poplar can provide both reduced recalcitrance and value-added lignin.

This study adds to a growing body of evidence which shows that any compounds that are compatible with radical coupling and that are present in the cell wall during lignin deposition can become incorporated into lignin (Ralph *et al.*, 2008b). In the case of the *QsuB*-poplar, the plants are clearly capable of producing and transporting DHB esters (and the various glycosylated conju-gates as well) to the cell wall for polymerization. These new monolignol–DHB conjugates offer another example of how engi-neering bioenergy crops can not only improve the efficiency of industrial biomass processing but also potentially increase the value of lignin as DHBA itself could be a valuable coproduct in future biorefineries.
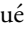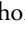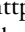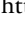
Author contributions

FU and SDM conceived the project, FU produced transgenic poplar lines, conducted wood chemistry analysis, and wrote the article with contributions from YM, ELM, and all the authors. YM performed microscopy analyses and provided technical assis-tance, data interpretation, and guidance. ELM conducted gene expression analysis and methanol extractions; SDK conducted liquid chromatography mass spectrometry (LC-MS) analyses and

provided technical assistance; KHK performed GPC, 2D-NMR, and biomass saccharification analysis. DL and AE created the expression construct and provided guidance for the project. JR synthesized the benzodioxane standard, analyzed NMR data, and supervised completion of the manuscript. SDM conceived the project, and supervised the experiments and completion of the manuscript.

ORCID

Aymerick Eudes https://orcid.org/0000-0002-1387-6111
Steven D. Karlen https://orcid.org/0000-0002-2044-8895
Kwang Ho Kim https://orcid.org/0000-0003-3943-1927
Dominique Loqué https://orcid.org/0000-0002-2060-6611
Elizabeth L. Mahon https://orcid.org/0000-0002-5177-7018
Shawn D. Mansfield https://orcid.org/0000-0002-0175-554X
Yaseen Mottiar https://orcid.org/0000-0002-4106-6159
John Ralph https://orcid.org/0000-0002-6093-4521
Faride Unda https://orcid.org/0000-0003-0842-8741

Data availability

All data supporting the findings of this study are available in the Supporting Information or available from the corresponding author upon request.

References

Barakat A, Choi A, Yassin NBM, Park JS, Sun Z, Carlson JE. 2011. Comparative genomics and evolutionary analyses of the *O*-methyltransferase gene family in *Populus*. *Gene* 479: 37–46.

Beckham GT, Johnson CW, Karp EM, Salvachúa D, Vardon DR. 2016. Opportunities and challenges in biological lignin valorization. *Current Opinion in Biotechnology* 42: 40–53.

Bjurhager I, Olsson A, Zhang B, Gerber L, Kumar M, Berglund LA, Burget I, Sundberg B, Salmen L. 2010. Ultrastructure and mechanical properties of *Populus* wood with reduced lignin content caused by transgenic down-regulation of cinnamate 4-hydroxylase. *Biomacromolecules* 11: 2359–2365.

Boerjan W, Ralph J, Baucher M. 2003. Lignin biosynthesis. *Annual Review of Plant Biology* 54: 519–546.

Bonawitz ND, Chapple C. 2010. The genetics of lignin biosynthesis: connecting genotype to phenotype. *Annual Review of Genetics* 44: 337–363.

Codignola A, Verotta L, Spanu P, Maffei M, Scannerini S, Bonfante-Fasolo P. 1989. Cell wall bound-phenols in roots of vesicular-arbuscular mycorrhizal plants. *New Phytologist* 112: 221–228.

Coleman HD, Park J, Nair R, Chapple C, Mansfield SD. 2008a. RNAi-mediated suppression of *p*-coumaroyl-CoA 3′-hydroxylase in hybrid poplar impacts lignin deposition and soluble secondary metabolism. *Proceedings of the National Academy of Sciences, USA* 105: 4501–4506.

Coleman HD, Samuels AL, Guy RD, Mansfield SD. 2008b. Perturbed lignification impacts tree growth in hybrid poplar—a function of sink strength, vascular integrity, and photosynthetic assimilation. *Plant Physiology* 148: 1229–1237.

Eudes A, George A, Mukerjee P, Kim JS, Pollet B, Benke PI, Yang F, Mitra P, Sun L, Cetinkol OP et al. 2012. Biosynthesis and incorporation of side-chain-truncated lignin monomers to reduce lignin polymerization and enhance saccharification. *Plant Biotechnology Journal* 10: 609–620.

Eudes A, Pereira JH, Yogiswara S, Wang G, Teixeira Benites V, Baidoo EE, Lee TS, Adams PD, Keasling JD, Loqué D. 2016. Exploiting the substrate promiscuity of hydroxycinnamoyl-CoA: shikimate hydroxycinnamoyl transferase to reduce lignin. *Plant and Cell Physiology* 57: 568–579.

Eudes A, Sathitsuksanoh N, Baidoo EEK, George A, Liang Y, Yang F, Mitra P, Sun L, Cetinkol O, Bhabout S et al. 2015. Expression of a bacterial 3-dehydroshikimate dehydratase reduces lignin content and improves biomass saccharification efficiency. *Plant Biotechnology Journal* 13: 1241–1250.

Finkle BJ, Masri MS. 1964. Methylation of polyhydroxyaromatic compounds by pampas grass *O*-methyltransferase. *Biochimica et Biophysica Acta* 85: 167.

Freudenberg K, Neish AC. 1968. *Constitution and biosynthesis of lignin.* Berlin & Heidelberg, Germany; New York, NY, USA: Springer-Verlag.

Goacher RE, Mottiar Y, Mansfield SD. 2021. ToF-SIMS imaging reveals that *p*-hydroxybenzoate groups specifically decorate the lignin of fibres in the xylem of poplar and willow. *Holzforschung* 75: 452–462.

Hao Z, Yogiswara S, Wei T, Benites VT, Sinha A, Wang G, Baidoo EEK, Ronald PC, Scheller HV, Loqué D et al. 2021. Expression of a bacterial 3-dehydroshikimate dehydratase (*QsuB*) reduces lignin and improves biomass saccharification efficiency in switchgrass (*Panicum virgatum* L.). *BMC Plant Biology* 21: 56.

Joshi CR, Thammannagowda S, Fujino T, Gou JQ, Avci U, Haigler CH, McDonnell LM, Mansfield SD, Mengesha B, Carpita NC et al. 2011. Perturbation of wood cellulose synthesis causes pleiotropic effects in transgenic aspen. *Molecular Plant* 4: 331–345.

Karlen SD, Zhang C, Peck ML, Smith RA, Padmakshan D, Helmich KE, Free HCA, Lee S, Smith BG, Lu F et al. 2016. Monolignol ferulate conjugates are naturally incorporated into plant lignins. *Science Advances* 2: 1–9.

Kim H, Li Q, Karlen SD, Smith RA, Shi R, Liu J, Yang C, Tunlaya-Anukit S, Wang J, Chang HM et al. 2020. Monolignol benzoates incorporate into the lignin of transgenic *Populus trichocarpa* depleted in C3H and C4H. *ACS Sustainable Chemistry & Engineering* 8: 3644–3654.

Kim H, Ralph J, Yahiaoui N, Pean M, Boudet AM. 2000. Cross-coupling of hydroxycinnamyl aldehydes into lignins. *Organic Letters* 2: 2197–2200.

Kim H, Ralph J, Lu F, Ralph SA, Boudet AM, MacKay JJ, Sederoff RR, Ito T, Kawai S, Ohashi H et al. 2003. NMR analysis of lignins in CAD-deficient plants. Part 1. Incorporation of hydroxycinnamaldehydes and hydroxybenzaldehydes into lignins. *Organic & Biomolecular Chemistry* 1: 268–281.

Kim H, Ralph J. 2010. Solution-state 2D NMR of ball-milled plant cell wall gels in DMSO-d_6/pyridine-d_5. *Organic & Biomolecular Chemistry* 8: 576–591.

Kupče E, Freeman R. 1997. Compensated adiabatic inversion pulses: broadband INEPT and HSQC. *Journal of Magnetic Resonance* 187: 258–265.

Kuroda H. 1983. Comparative studies on *O*-methyltransferases involved in lignin biosynthesis. *Wood Research: Bulletin of the Wood Research Institute Kyoto University* 69: 91–135.

Lam KC, Ibrahim RK, Behdad B, Dayanandan S. 2007. Structure, function, and evolution of plant *O*-methyltransferases. *Genome* 50: 1001–1013.

Lan W, Lu F, Regner M, Zhu Y, Rencoret J, Ralph S, Zakai U, Morreel K, Boerjan W, Ralph J. 2015. Tricin, a flavonoid monomer in monocot lignification. *Plant Physiology* 167: 1284–1295.

Leplé J-C, Dauwe R, Morreel K, Storme Véronique, Lapierre C, Pollet B, Naumann A, Kang K-Y, Kim H, Ruel K et al. 2007. Downregulation of cinnamoyl-coenzyme A reductase in poplar: multiple-level phenotyping reveals effects on cell wall polymer metabolism and structure. *Plant Cell* 19: 3669–3691.

Li L, Zhou Y, Cheng X, Sun J, Marita JM, Ralph J, Chiang V. 2003. Combinatorial modification of multiple lignin traits in trees through multigene co-transformation. *Proceedings of the National Academy of Sciences, USA* 100: 4939–4944.

Liang D, Hao Z, Liu Y, Luo H, Wang Y, Zhang C, Zhang Q, Chen R, Yu D. 2013. Bioactive carboxylic acids from *Lysimachia clethroides*. *Journal of Asian Natural Products Research* 15: 59–66.

Loscher R, Heide L. 1994. Biosynthesis of *p*-hydroxybenzoate from *p*-coumarate and *p*-coumaroyl-coenzyme A in cell-free extracts of *Lithospermum erythrorhizon* cell cultures. *Plant Physiology* 106: 271–279.

Lu F, Karlen SD, Regner M, Kim H, Ralph SA, Sun R, Kuroda K, Augustin MA, Mawson R, Sabarez H et al. 2015. Naturally *p*-hydroxybenzoylated lignins in palms. *Bioenergy Research* 8: 934–952.

Lu F, Ralph J. 2002. Preliminary evidence for sinapyl acetate as a lignin monomer in kenaf. *JCS Chemical Communications* 1: 90–91.

Mahon EL, Mansfield SD. 2019. Tailor-made trees: engineering lignin for ease of processing and tomorrow's bioeconomy. *Current Opinion in Biotechnology* **56**: 147–155.

Mahon EL, de Vries L, Jang S, Middar S, Kim H, Unda F, Ralph J, Mansfield SD. 2021. Expression of an exogenous chalcone synthase in poplar developing xylem results in the novel incorporation of naringenin in lignins. *Plant Physiology* **188**: 984–996.

Mansfield S, Kim H, Lu F, Ralph J. 2012. Whole plant cell wall characterization using solution-state 2D NMR. *Nature Protocols* **7**: 1–11.

Mottiar Y, Vanholme R, Boerjan W, Ralph J, Mansfield SD. 2016. Designer lignins: harnessing the plasticity of lignification. *Current Opinion in Biotechnology* **37**: 190–200.

Murphy EK, Mottiar Y, Soolanayakanahally RY, Mansfield SD. 2021. Variations in cell wall traits impact saccharification potential of *Salix famelica* and *Salix eriocephala*. *Biomass & Bioenergy* **148**: 106051.

Nakamura Y, Higuchi T. 1976. Ester linkage of *p*-coumaric acid in bamboo lignin. *Holzforschung* **30**: 187–191.

Ralph J. 2010. Hydroxycinnamates in lignification. *Phytochemistry Reviews* **9**: 65–83.

Ralph J, Brunow G, Harris PJ, Dixon RA, Schatz PF, Boerjan W. 2008a. Lignification: are lignins biosynthesized via simple combinatorial chemistry or via proteinaceous control and template replication? In: Daayf F, El Hadrami A, Adam L, Ballance GM, eds. *Recent advances in polyphenol research, vol. 1.* Oxford, UK: Wiley-Blackwell Publishing, 36–66.

Ralph J, Kim H, Lu F, Grabber JH, Leplé J, Berrio-Sierra J, Derikvand MM, Jouanin L, Boerjan W, Lapierre C. 2008b. Identification of the structure and origin of a thioacidolysis marker compound for ferulic acid incorporation into angiosperm lignins (and an indicator for cinnamoyl CoA reductase deficiency). *The Plant Journal* **53**: 368–379.

Ralph J, Lapierre C, Marita JM, Kim H, Lu F, Hatfield RD, Ralph S, Chapple C, Franke R, Hemm MR *et al.* 2001. Elucidation of new structures in lignins of CAD- and COMT-deficient plants by NMR. *Phytochemistry* **57**: 993–1003.

Ralph J, Lundquist K, Brunow G, Lu F, Kim H, Schatz PF, Marita JM, Hatfield RD, Ralph SA, Christensen JH *et al.* 2004. Lignins: natural polymers from oxidative coupling of 4-hydroxyphenylpropanoids. *Phytochemistry Reviews* **3**: 29–60.

Ralph J, Lu F. 1998. The DFRC method for lignin analysis. A simple modification for identifying natural acetates on lignins. *Journal of Agricultural and Food Chemistry* **46**: 4616–4619.

Rencoret J, Neiva D, Marques G, Gutiérrez A, Kim H, Gominho J, Pereira H, Ralph J, del Río JC. 2019. Hydroxystilbene glucosides are incorporated into Norway spruce bark lignin. *Plant Physiology* **180**: 1310–1321.

del Río JC, Rencoret J, Gutierrez A, Elder T, Kim H, Ralph J. 2020. Lignin monomers from beyond the canonical monolignol biosynthetic pathway: another brick in the wall. *ACS Sustainable Chemistry & Engineering* **8**: 4997–5012.

del Río JC, Rencoret J, Gutiérrez A, Kim H, Ralph J. 2018. Structural characterization of lignin from maize (*Zea mays* L.) fibers: evidence for diferuloylputrescine incorporated into the lignin polymer in maize kernels. *Journal of Agricultural and Food Chemistry* **66**: 4402–4413.

del Río JC, Rencoret J, Prinsen P, Martínez AT, Ralph J, Gutiérrez A. 2012. Structural characterization of wheat straw lignin as revealed by analytical pyrolysis, 2D-NMR, and reductive cleavage methods. *Journal of Agricultural and Food Chemistry* **60**: 5922–5935.

Schuster B, Winter M, Herrmann K. 1986. 4-O-β-ᴅ-Glucosides of hydroxybenzoic and hydroxycinnamic acids — their synthesis and determination in berry fruit and vegetable. *Zeitschrift Für Naturforschung C: A Journal of Biosciences* **41**: 511–520.

Sederoff RR, MacKay JJ, Ralph J, Hatfield RD. 1999. Unexpected variation in lignin. *Current Opinion in Plant Biology* **2**: 145–152.

Sircar D, Mitra A. 2008. Evidence for *p*-hydroxybenzoate formation involving enzymatic phenylpropanoid side-chain cleavage in hairy roots of *Daucus carota*. *Journal of Plant Physiology* **165**: 407–414.

Van Acker R, Leplé J-C, Aerts D, Storme V, Goeminne G, Ivens B, Légée F, Lapierre C, Piens K, Van Montagu MCE *et al.* 2014. Improved saccharification and ethanol yield from field-grown transgenic poplar deficient in cinnamoyl-CoA reductase. *Proceedings of the National Academy of Sciences, USA* **111**: 845–850.

Vanholme R, Morreel K, Darrah C, Oyarce P, Grabber JH, Ralph J, Boerjan W. 2012. Metabolic engineering of novel lignin in biomass crops. *New Phytologist* **196**: 978–1000.

de Vries L, Guevara-Rozo S, Cho M, Liu L, Renneckar S, Mansfield SD. 2021. Tailoring renewable materials via plant biotechnology. *Biotechnology for Biofuels* **14**: 167.

de Vries L, MacKay HA, Smith RA, Mottiar Y, Karlen SD, Unda F, Muirragui E, Bingman C, Vander Meulen K, Beebe ET *et al.* 2022. *p*HBMT1, a BAHD-family monolignol acyltransferase, mediates lignin acylation in poplar. *Plant Physiology* **188**: 1014–1027.

Wang JP, Matthews ML, Williams CM, Shi R, Yang C, Tunlaya-Anukit S, Chen HS, Li Q, Liu J, Lin CY *et al.* 2018. Improving wood properties for wood utilization through multi-omics integration in lignin biosynthesis. *Nature Communications* **9**: 1579.

Wang JP, Naik PP, Chen H, Shi R, Lin C, Liu J, Shuford CM, Li Q, Sun YH, Tunlaya-Anukit S *et al.* 2014. Complete proteomic-based enzyme reaction and inhibition kinetics reveal how monolignol biosynthetic enzyme families affect metabolic flux and lignin in *Populus trichocarpa*. *Plant Cell* **26**: 894–914.

Wang Z, Gao H, Yang C, Sun Z, Wu L. 2011. Novel cyanoglucosides from the leaves of *Hydrangea macrophylla*. *Helvetica Chimica Acta* **94**: 847–852.

Weber B, Hoesch L, Rast DM. 1995. Protocatechualdehyde and other phenols as cell wall components of grapevine leaves. *Phytochemistry* **40**: 433–437.

Wilkerson CG, Mansfield SD, Lu F, Withers S, Park JY, Karlen SD, Gonzales-Vigil E, Padmakshan D, Unda F, Rencoret J *et al.* 2014. Monolignol ferulate transferase introduces chemically labile linkages into the lignin backbone. *Science* **344**: 90–93.

Wu W, Dutta T, Varman AM, Eudes A, Manalansan B, Loqué D, Singh S. 2017. Lignin valorization: two hybrid biochemical routes for the conversion of polymeric lignin into value-added chemicals. *Scientific Reports* **7**: 8420–8513.

Xie N, Liang H, Huang R, Xu P. 2014. Biotechnological production of muconic acid: current status and future prospects. *Biotechnology Advances* **32**: 615–622.

Yamanaka M, Shimomura K, Sasaki K, Yoshihira K. 1995. Glucosylation of phenolics by hairy root cultures of *Lobelia sessilifolia*. *Phytochemistry* **40**: 1149–1150.

Zhao Y, Yu X, Lam P-Y, Zhang K, Tobimatsu Y, Liu C-J. 2021. Monolignol acyltransferase for lignin *p*-hydroxybenzoylation in *Populus*. *Nature Plants* **7**: 1288–1300.

Ziebell A, Gracom K, Katahira R, Chen F, Pu Y, Ragauskas A, Dixon RA, Davis M. 2010. Increase in 4-coumaryl alcohol units during lignification in alfalfa (*Medicago sativa*) alters the extractability and molecular weight of lignin. *Journal of Biological Chemistry* **285**: 38961–38968.

Supporting Information

Additional Supporting Information may be found online in the Supporting Information section at the end of the article.

Fig. S1 Transcript abundance of the bacterial 3-dehydroshiki-mate dehydratase *QsuB* in the developing xylem of hybrid poplar.

Fig. S2 Comparison of growth phenotype.

Fig. S3 Comparison of air-dried stem sections of wild-type poplar and *QsuB*-poplar line 1.

Fig. S4 Representative transversal cross-sections of poplar xylem stained with phloroglucinol-HCl and toluidine-blue of *QsuB*-poplar line 1 and wild-type poplar.

Fig. S5 Ultrahigh-pressure liquid chromatography (UHPLC) traces of alkaline hydrolysates of extractive-free wood from *QsuB*-poplar line 1 and wild-type poplar.

Fig. S6 UV-visible spectra of compounds released by alkaline hydrolysis of extractive-free stem tissue of *QsuB*-poplar line 1.

Fig. S7 Two-dimensional heteronuclear single-quantum coherence (HSQC) NMR spectra profiling the isolated enzyme-lignins from wild-type poplar and *QsuB*-poplar line 15.

Fig. S8 Preparation of the radical cross-coupling benzodioxane product BD between methyl DHB MDHB and coniferyl alcohol M as a model to obtain chemical shifts for the analogous structure in lignin HSQC spectra.

Fig. S9 Pathway diagram depicting the biosynthesis of DHBA from 3-dehydroshikimate, an intermediate of the shikimate pathway, as well as the production of DHB–monolignol conjugates, 4-hydroxy-3-methoxybenzoate, 3-hydroxy-4-methoxybenzoate, and various related glycosides.

Methods S1 Generation, selection, and cultivation of transgenic hybrid poplar, as well as cell wall composition, wood density, lignin histology, and the synthesis of benzodioxane model compound.

Table S1 Phenotypic characterizations, wood density and biomass of stem of 5-month-old glasshouse-grown *QsuB*-poplar and wild-type trees.

Please note: Wiley Blackwell are not responsible for the content or functionality of any Supporting Information supplied by the authors. Any queries (other than missing material) should be directed to the *New Phytologist* Central Office.

About *New Phytologist*

- *New Phytologist* is an electronic (online-only) journal owned by the New Phytologist Foundation, a **not-for-profit organization** dedicated to the promotion of plant science, facilitating projects from symposia to free access for our Tansley reviews and Tansley insights.

- Regular papers, Letters, Viewpoints, Research reviews, Rapid reports and both Modelling/Theory and Methods papers are encouraged. We are committed to rapid processing, from online submission through to publication 'as ready' via *Early View* – our average time to decision is <23 days. There are **no page or colour charges** and a PDF version will be provided for each article.

- The journal is available online at Wiley Online Library. Visit **www.newphytologist.com** to search the articles and register for table of contents email alerts.

- If you have any questions, do get in touch with Central Office (np-centraloffice@lancaster.ac.uk) or, if it is more convenient, our USA Office (np-usaoffice@lancaster.ac.uk)

- For submission instructions, subscription and all the latest information visit **www.newphytologist.com**